




Article

Impact of Climate Change on the Phenology of Winter Oilseed Rape (*Brassica napus* L.)

Jürgen Junk ^{1,*}, Arturo Torres ², Moussa El Jaroudi ³ and Michael Eickermann ¹

¹ Environmental Research and Innovation, Luxembourg Institute of Science and Technology, 4422 Luxembourg, Luxembourg; michael.eickermann@list.lu

² Helmholtz-Zentrum Hereon, Climate Service Center Germany (GERICS), Fischertwiete 1, 20095 Hamburg, Germany; jairo.torres@hereon.de

³ Water, Environment and Development Unit, SPHERES Research Unit, Department of Environmental Sciences and Management, University of Liège, 6700 Arlon, Belgium; meljaroudi@uliege.be

* Correspondence: juergen.junk@list.lu; Tel.: +352-275-888 (ext. 5011)

Abstract: In our investigation, we have developed innovative statistical models tailored to predict specific phenological stages of winter oilseed rape (WOSR) cultivation in Luxembourg. Leveraging extensive field observations and meteorological data, our modeling approach accurately forecasts critical growth stages of WOSR, including inflorescence emergence (BBCH 51), initial flowering (BBCH 60), and cessation of flowering (BBCH 69), capitalizing on accumulated heat units. Our findings challenge conventional assumptions surrounding base temperatures, advocating for a specific base temperature of 3 °C for winter oilseed rape emergence, consistent with prior research. Validation via leave-one-out cross-validation yields promising outcomes, with average Root Mean Square Error (RMSE) values below 1, surpassing analogous studies. Particularly noteworthy is our model's performance in predicting crucial growth stages, notably BBCH 60, pivotal for pest control. Despite advancements, hurdles persist in forecasting late-stage phenological events influenced by leaf senescence and anticipated climate change impacts, likely accelerating WOSR development and introducing new risks. In response, cultivar selection strategies informed by individual development rates and temperature sensitivities emerge as vital mitigation measures. As climate variability intensifies, precision agriculture assumes paramount importance in optimizing resource allocation and ensuring sustainable WOSR cultivation practices. Our study advocates for proactive integration of predictive modeling into adaptive management frameworks, empowering stakeholders to make informed decisions taking climatic dynamics into account.

Keywords: growth stages; climate change impact assessment; oilseed rape; regional climate change projections; PMP5.5 modeling platform



Citation: Junk, J.; Torres, A.; El Jaroudi, M.; Eickermann, M. Impact of Climate Change on the Phenology of Winter Oilseed Rape (*Brassica napus* L.). *Agriculture* **2024**, *14*, 1049. <https://doi.org/10.3390/agriculture14071049>

Academic Editor: Dengpan Xiao

Received: 26 May 2024

Revised: 22 June 2024

Accepted: 25 June 2024

Published: 29 June 2024



Copyright: © 2024 by the authors. Licensee MDPI, Basel, Switzerland. This article is an open access article distributed under the terms and conditions of the Creative Commons Attribution (CC BY) license (<https://creativecommons.org/licenses/by/4.0/>).

1. Introduction

The EU total oilseed area is expected to reach 11.3 million ha in 2026 [1]. While oilseed yields for sunflower and soybeans are projected to increase, the situation for winter oilseed rape (*Brassica napus* L., WOSR) is more demanding, because it is highly sensitive to unfavorable weather conditions and pest pressure [2]. Besides those challenges, WOSR has significant socioeconomic importance and several advantages for cropping systems such as erosion protection, high yields, and breaking of grain-based crop rotations [3–5]. Nevertheless, WOSR requires an intensive management of fertilizers as well as pesticide application to control diseases and insect pests [6]. Environmental changes like increased air temperatures and changes in precipitation patterns will also affect biomass production [7,8], yield, as well as the characteristic phenology of WOSR and its associated pest [9]. Climate projections indicate a potential temperature rise from 3 °C to 5 °C, depending on the emission scenario, until the end of the 21st century [10]. Increased temperatures due to climate change will highly impact the growth and yield of agricultural crops, for instance

leading to shorter crop rotations [11,12]. While Borges et al. [13] expect shifts concerning areas that are suitable for cultivation of WOSR under climate change, the increasing variability in meteorological extreme events such as droughts and heat waves [14,15] will influence the growing conditions for WOSR as well as leading to the need for developing adaptive management strategies and decision support tools for ecological intensification of this crop [7].

Regional climate change predictions based on multi-model ensemble approaches are suitable tools to assess the impact of possible future climate realizations on the local scale [14,16–21]. Air temperatures in Luxembourg have significantly increased during the 20th century [14]. Studies about modeling the response of rapeseed phenology in a climate change context are scarce [7,19,20], but necessary for predicting the plant performance under different future climate conditions.

The general response of plants to temperature can be modeled by chilling (cool temperatures) and forcing models (warm temperatures). Depending on the applied model, the accuracy of the predicted phenology is linked to different levels of uncertainties [21]. Such models are usually calibrated using phenological observations from a single site or a collection of sites as it is widely carried out for grapevine phenology [22,23]. Non-linear models describe the complex relationship between temperature and crop development based on thermal kinetic conditions. These models normally include temperature thresholds for optimal plant development. Temperatures above or below these thresholds hamper the development of the plants [24].

In the present study, we used the Phenology Modelling Platform Version 5.5 [25] to define models for the simulation of the cardinal growth stages of WOSR (beginning of inflorescence emergence, beginning of flowering and end of flowering). These growth stages are of significant importance for phytosanitary aspects, being highly associated with several insect pests of economic impact [26]. The pollen beetle, *Brassicogethes aeneus*, is the major pest in WOSR causing damages on young flowering buds leading to a decrease in the yield of up to 70% [27]. Currently, chemical control by insecticide applications is common in the growth stages 51 to 59. This strategy fosters the development of insecticide resistance [28]. With the beginning of flowering (BBCH 60), the pollen beetle can reach the pollen of already open flowers as a food resource avoiding further damage to the plant. Therefore, expert knowledge of plant phenology is crucial for the appropriate control of relevant pests in WOSR. Even by using decision support tools to forecast the migration of *Brassicogethes aeneus* [9], side effects by chemical applications to non-target organisms in WOSR are still possible. While WOSR has a high melliferous potential [29] pollinator species are mostly common in this crop and can be highly affected by insecticide applications [30]. Forecast systems giving information on the current phenological stage can be helpful tools to assist the farmer in timing the pesticide applications to guarantee ecological intensification. So far, some phenological models have been developed in WOSR [31–33] focusing on biomass allocation as well as seed yield and quality but were rarely used as decision support tools.

The main objectives of the present study are twofold: (a) to quantify the accuracy of the model in the simulation of the cardinal phenological stages of rapeseed in Luxembourg based on a long-term observational data set (2007–2019); and (b) to evaluate the impact of projected changes in air temperatures on these stages based on a multi-model and multi emission scenario approach.

2. Materials and Methods

2.1. Phenological Observations and Meteorological Measurements

The data used in this study were collected from field trials conducted over several years and in multiple locations, observing the phenology of different winter cultivars of WOSR. The cultivars varied between years and locations, but all were winter cultivars. To record the phenological stages, observations were made every three days from 2007 to 2019 at different sites. The key by Meier [34] was used to identify the phenological stages. For

this study, we have chosen the site at Remich [49° 54'; 6° 36'; 160 m AMSL] as a typical region for the growth of WOSR in Luxembourg. The sites were continuously monitored, starting from the inflorescence emergence (also known as the green bud stage BBCH 51), through initial flowering (BBCH 60) up to the end of flowering (BBCH 69). One hundred individual plants were randomly selected, the growth stage of each plant was determined and then the mean growth stage of all plants was calculated, following the methodology outlined by Lancashire et al. [35].

In conjunction with field observations, meteorological data were gathered from standard automatic weather stations (AWSs) administered by the “Administration des Services Techniques de l’Agriculture” (ASTA). Situated within a radius of less than three kilometers from the WOSR fields, these AWSs provided precise data crucial for our study. The datasets encompassed various meteorological parameters, including air temperature, precipitation, wind speed, and cloud cover. To ensure data accuracy and reliability, an automated data processing chain was used. This chain was tasked with identifying data gaps, plausibility control, and interpolating missing values. Those quality-controlled datasets are the basis for the development of the phenological models.

2.2. Climate Change Projections and Bias Correction

The phenological model was driven by time series obtained from a multi-model ensemble of climate change projections taken from the Coordinated Regional Climate Downscaling Experiment (CORDEX), which is a part of the World Climate Research Programme (WCRP). The aim of EURO-CORDEX is to provide climate change information at the regional level. To achieve this, daily values of minimum, maximum, and mean air temperature were extracted for three Representative Concentration Pathways (RCPs) namely the RCP2.6, RCP4.5, and RCP8.5. Hence, we want to include the RCP2.6 scenario in our study the number of available ensemble members was comparable low. The dataset used in this study comprises transient model simulations spanning from 1971 to 2091. To evaluate the projected levels of changes in basic meteorological variables, we retrieved time series data of daily maximum and minimum air temperature from a partially stored version of the EURO-CORDEX data repository. The models utilized in our analysis are listed in Table 1.

Table 1. Regional climate change projections with model abbreviations, the driving global climate model (GCM), the regional climate model (RCM) used for the dynamical downscaling as well as the institutions that are responsible for the model runs; temporal resolution: daily data; time span: 1971–2091.

Model Number	Official CMIP5 GCM Name	Modelling Centre/Group CMIP5 Institute ID	Official EURO CORDEX RCM Name	Modelling Centre EURO-CORDEX Institute ID
M3	HadGEM2-ES	CNRM MOHC	RACMO22E	KNMI
M4	HadGEM2-ES	CNRM MOHC	RCA4	SMHI
M5	MPI-ESM-LR	MPI-M	REMO2009	MPI-CSC
M6	MPI-ESM-LR	MPI-M	RCA4	SMHI

A non-parametric quantile mapping technique was utilized to rectify biases in climate model outputs by adjusting their distribution to align with the observed data from the World Meteorological Organization (WMO) station and Findel airport in Luxembourg (WMO ID = 06590). This method involves transforming the cumulative distribution function (CDF) of the model output to match the CDF of the observed data through empirical quantiles, without specifying a parametric form for the distributions. Firstly, the corresponding model output and observed data are sorted separately in ascending order [36]. Then, the empirical CDFs of the model output and observed data based on their respective rankings are calculated. Subsequently, the quantile mapping function is calculated by

matching the empirical quantiles of the model output with those of the observed data. Specifically, for each quantile value, such as the 10th percentile, the corresponding observed data value is matched with the model output value. The mapping function is obtained by interpolating between these pairs of quantiles [37]. Finally, the quantile mapping function is applied to the transient time series of air temperature to correct the bias. The flexibility of this method allows for the correction of biases across the entire distribution of the model output, rather than just at specific quantiles. The implementation of this method is carried out using the R programming language for statistical computing [38], with the aid of the R-package “qmap” [39].

2.3. Phenological Model

The simulation of phenological stages was carried out using process-based models that were constructed based on temperature conditions and photoperiods. The selection and fitting of the models were performed using the freely available Phenology Modelling Platform PMP5.5 [25], wherein an iterative testing process was utilized to determine the best-fit model parameters that optimize the climatic requirements for the development of WOSR. The estimation of the best-fit parameters is based on the method described by Metropolis et al. [40]. Instead of defining one model for the three different phenological stages, we defined individual models for each stage. The individual models overperformed in terms of Root Mean Square Error (*RMSE*) and model efficiency (*EFF*), with a single model for all stages. For the beginning of the inflorescence emergence (BBCH 51), a triangular function with three parameters T_{minimum} , T_{optimum} , and T_{maximum} , where T_{optimum} represents the optimal temperature from which the accumulated amount of heat units begins to decline, was used. Further details for this function are given by Hänninen [41]. For the initial flowering (BBCH 60), the implemented function in the PMP5 model platform of Richardson et al. [42] was used. It is a modified version of the growing degree day function with a plateau above the threshold parameter T_{high} . For the last stage investigated in our study, namely the end of flowering (BBCH 69), a parabolic function was used. This function was described by Chuine and Beaubien [43] and is based on the photosynthetic activity, has only one parameter T_{optimum} and consists of implemented by a third-order polynomial function. Further details including graphical representation of the three functions used in this study can be found in the manual of the PMP5.5 modeling platform.

2.4. Model Validation and Statistics

The model performance was assessed based on the Root Mean Square Error (*RMSE*) (1) and the model efficiency (*EFF*) (2), which explains the percentage of variance.

$$RMSE = \sqrt{\frac{\sum_{i=1}^N (x_{a,i} - x_{b,i})^2}{N}} \quad (1)$$

For the *RMSE*, x_a refers to the observed day of the phenological stage, x_b to the simulated day of the phenological stage and N to the number of observations.

$$EFF = \frac{(x_{a,i} - \bar{x}_{a,i})^2 - (x_{a,i} - \bar{x}_{b,i})^2}{(x_{a,i} - \bar{x}_{a,i})^2} \quad (2)$$

The *EFF* varies between $-\infty$ and $+1$, with $+1$ describing a perfect fit between observed and estimated data, explaining more variance than the null model (average) with relates to zero corresponding; and \bar{x} = averaged observed day of the phenological stage. Negative *EFF* values indicate that the model performed worse than the null model. The variability between observed and simulated days was identified by using the determination coefficient (R^2).

To check the quality of the model, the built-in function “leave-one-out cross-validation” of the PMP5.5 modeling platform was used. This automatically generates n subsequent

independent optimizations, where n is the number of data available to fit the model, using $n - 1$ data, i.e., excluding one data each time [44]. For the analysis of the future climate condition, the phenological stages were divided into three 30-year time spans: the reference scenario (1971–2000), the near future (2021–2050) and the far future scenario (2061–2090). The Kruskal–Wallis Analysis of Variance (ANOVA) on ranks was used to test the two future time spans for significant differences ($p < 0.001$) against the reference time span of 1971–2000 using the SigmaPlot Ver.10 from Systat Software, Inc. San Jose, CA, USA.

3. Results

3.1. Results of the Phenological Models

For each of the three phenological stages, individual models were constructed using the functionalities of the PMP5.5 modeling platform. The code for these models is provided in Appendices A–C as XML files, representing direct outputs from the modeling process (Appendix A for BBCH stage 51, Appendix B for BBCH stage 60, and Appendix C for BBCH stage 69). The outcomes of these individual models are depicted in Figure 1.

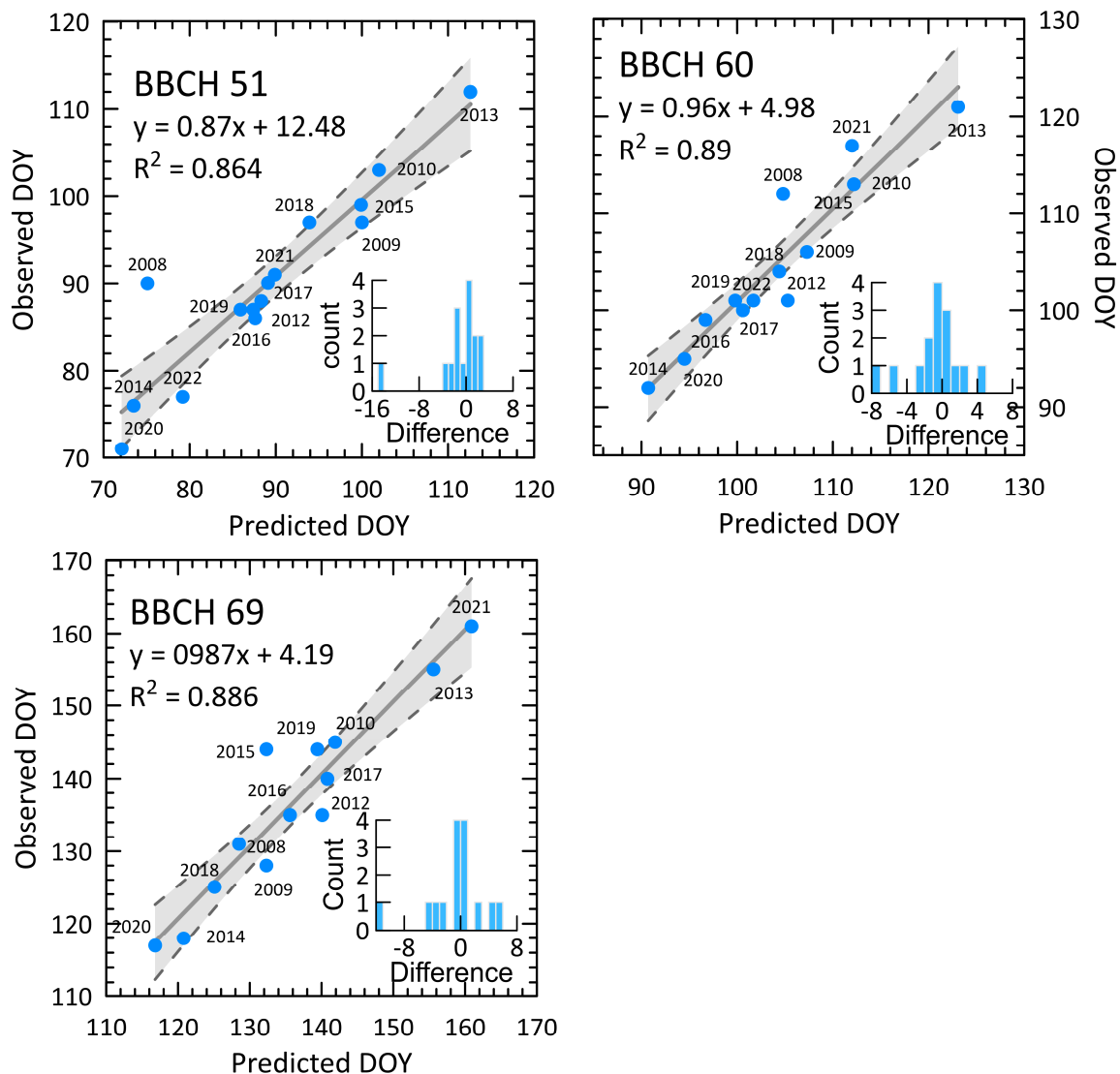


Figure 1. Predicted versus observed Day of Year (DOY) of BBCH 51, BBCH 60 and BBCH 69 based on the output of the PMP5.5 modeling platform driven by meteorological observation from 2007 to 2019 and field observations of the BBCH stages. Upper and lower dashed lines indicate a confidence interval (99%). The small histograms indicate the absolute frequencies between the measured and modeled data for each model.

For the initial BBCH stage, the mean predicted Day of Year (DOY) is 89.1, while the mean observed DOY across all years is 90.1 (R^2 : 0.864, mean $RMSE$: 0.67). The largest disparity between observed and predicted DOY was 14.9 days in 2008, whereas the smallest difference was 0.3 days in 2016. Notably, this 14.9-day difference is also the most significant among all three analyzed phenological stages. In 93% of cases, the differences between observed and predicted values did not exceed 3 days. Leave-one-out cross-validation revealed consistent results, with the lowest $RMSE$ value of 0.37 excluding the year 2008.

For BBCH stage 60, the mean predicted DOY is 104.6, compared to the mean observed DOY of 105.4 across all years (R^2 : 0.89, mean $RMSE$: 0.54). The highest difference, 7.2 days, was once again observed in 2008. In 79% of cases, disparities between observed and predicted values did not exceed 3 days.

Regarding the final stage (BBCH 69), the average modeled DOY was 136.1, compared to the mean observed DOY of 139.8 (R^2 : 0.886, $RMSE$: 0.8). Notably, the maximum difference of 11.7 days occurred in 2015, contrasting with previous stages. While all three predictive models generally exhibit a tendency to predict earlier growth stages than observed in the field, the disparities are evenly distributed, as illustrated by the histograms included in Figure 1.

3.2. Simulation of Future Phenological Stages

The dynamical downscaled multi-model ensemble approach yielded conclusive results on the impact of climate change on the phenological stages of WOSR. Using the PMP5.5 software, the selected stages were analyzed for the three different RCPs (RCP2.6, RCP4.5, and RCP8.5), with four ensemble members for input data. The reference period from 1971 to 2000 was compared to near and far future time spans of 30 years, and the results of the four ensemble member realizations of each RCP were pooled for further statistical analyses. Figure 2 displays boxplots of the results from the phenological modeling platform for each RCP and BBCH stage.

For BBCH stage 51, as shown in Figure 2 and Table 2, the reference period had a mean DOY of 96.3. The near future shows an earlier onset of the beginning of inflorescence emergence, with an average of 6 days earlier. In the far future, a further earlier onset is only observed for RCP4.5 and RCP8.5, as no further increase in the air temperature is projected until the end of this century for RCP2.6. For RCP4.5 and RCP8.5, a continuous shift towards an earlier onset of this stage was projected. These results provide clear evidence of the impact of climate change on the phenological stages of WOSR, highlighting the need for actions to mitigate those effects, because of increased frost risks in the near future.

Table 2. Multi model mean of the DOY of BBCH 51, 60 and 69 for the reference period 1971–2000 (R) near future 2021–2050 (NF) and far future 2061–2090 (FF) for the RCP2.6, RCP4.5 and RCP8.5. All differences between R, and NF, FF are statistically significant ($p < 0.001$).

BBCH Stage		RCP2.6			RCP4.5		RCP8.5	
		R	NF	FF	NF	FF	NF	FF
BBCH 51	Mean	97.17	92.17	91.085	91.61	89.21	90.67	84.43
	Variance	72.15	64.26	53.38	74.48	60.74	59.39	45.90
BBCH 60	Mean	116.25	111.22	110.06	111.00	107.64	110.69	103.50
	Variance	51.93	56.33	44.69	68.63	107.64	48.75	36.08
BBCH 69	Mean	146.51	142.68	142.98	142.57	140.90	142.98	140.40
	Variance	55.58	38.58	41.12	27.44	72.68	68.88	41.04

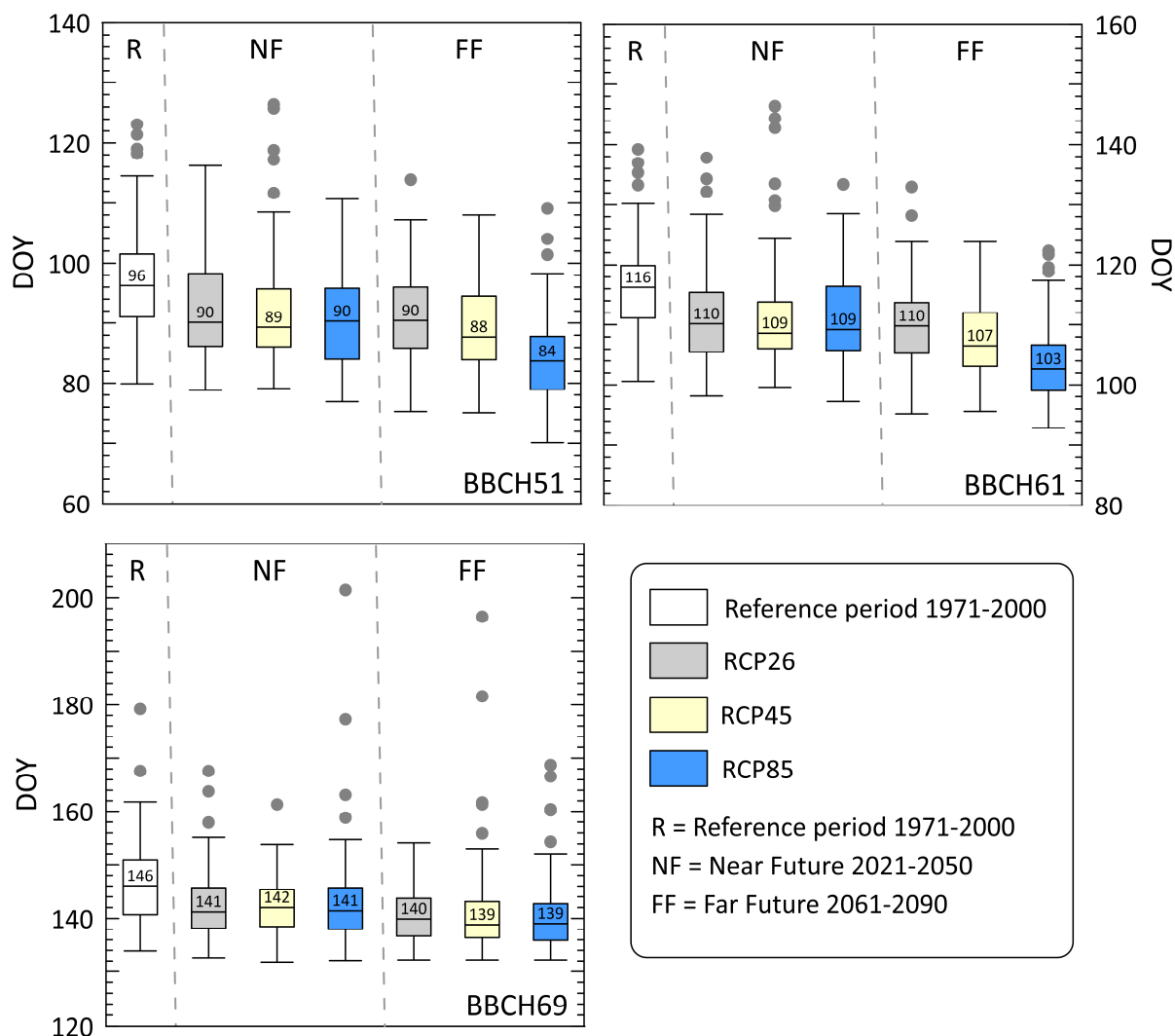


Figure 2. Boxplots of the three different BBCH stages for the climate change scenarios RCP2.6, RCP4.5 and RCP8.5, with the reference scenario, R (1971–2000), the near future, NF (2021–2050) and far future scenario, FF (2061–2090). The Boxplots were created as follows: The lower and upper hinges correspond to the first and third quartiles of the data. The upper and lower whisker extends from the hinge to the largest and lowest value no further than 1.5 times the Inter-Quartile Range. Data beyond the end of the whiskers are called ‘outlying’ points and are plotted individually as grey dots.

The BBCH stage 60 results display similar trends as the observed for BBCH stage 51. It is predicted that there will be a shift of six days for all RCPs in the near future, with only RCP8.5 showing a pronounced shift of an additional six days in the far future. These differences are statistically significant ($p < 0.05$) for all three RCPs. Figure 2 shows the overall pattern of the data, with marginal variations in the dates of BBCH 51 and BBCH 60 between the NF scenarios and RCP2.6 FF scenario. However, the far future RCP4.5 and RCP8.5 scenarios show stronger variations with medians ranging between 84 and 88 for BBCH 51 and 102 to 107 for BBCH 60. There are only slight differences between the medians for the climate scenarios for BBCH 69, with values ranging between 139 and 142.

4. Discussion

Utilizing extensive field data and corresponding meteorological records, we constructed statistical models to forecast distinct phenological stages of WOSR cultivation in Luxembourg. Through process-based modeling techniques, our analysis discerned the predictability of inflorescence emergence (BBCH 51), initial flowering (BBCH 60), and

cessation of flowering (BBCH 69) with high precision ($R^2 > 0.86$), relying on accumulated heat units as a key determinant. Notably, we pinpointed an optimal temperature range of 11.2 °C to 12.7 °C (T_{optimum}) for these critical growth stages, underscoring the physiological significance of this temperature window in shaping WOSR phenological development. Other studies [3,7] used considerably lower base temperatures of 3 °C or 5 °C which were applied for all phenological stages. According to Marshall and Squire [45], the optimal base temperature for the emergence of winter oilseed rape is 3 °C. Consequently, these threshold temperatures could rather represent an optimum for the model predictions than for the underlying processes of a phenological stage or be specifically relevant for stages of the plant development of BBCH 51 and higher. While in our approach soil temperature was not considered due to a lack of those measurements at the ASTA stations, this parameter was investigated by Drebenstedt et al. [8]. They described an acceleration of development during spring by increased soil temperatures. Precipitation was not considered because the relatively deep root system of WOSR makes it rather resilient to normal drought stress conditions [7].

The outcomes derived from the PMP5.5 modeling platforms demonstrate a satisfactory level of performance, proven by the alignment of model outputs with field observations. Notably, our analysis reveals average *RMSE* values below 1, indicative of a slight improvement over analogous investigations. Farré et al. [46] calculated the beginning of flowering of canola by using the APSIM model with an *RMSE* of 4.7 days. It is important to note that for the growth stage BBCH 60, which is of the highest relevance for controlling the pollen beetle because no further chemical applications are allowed, our model showed a very good performance. Furthermore, for the benchmark of the model performance, the uncertainty due to the frequency of growth stage observations in the fields of 3 days must be considered.

As described in other studies the predictions were less accurate for the phenological stage BBCH 69 (end of flowering). This might be attributed to the fact that in the later growth stages, most of the leaves on the terminal raceme are lost due to senescence by translocation of nitrogen to the already developing pods and no longer contribute to the photosynthetic activity of the plant [32,47]. According to Morrison et al. [48] increasing air temperature led to increases in the maximum individual leaf area. Due to the photosynthesis gap and corresponding changes in plant chemistry, air temperature is no longer the key driver for phenological development [49]. The problem of modeling the effect of leaf senescence was already discussed by Gabrielle et al. [32].

According to studies of Pullens et al. [7], and Junk et al. [14,15], the region of Luxembourg will face significantly higher air temperatures, especially when taking the RCP8.5 scenario into account. The benefit of elevated air temperature conditions might be a higher availability of nutrients and therefore promotion of biomass production [50]. Consequently, higher air temperatures during early phenological stages could accelerate the plant development, making WOSR more vulnerable to low temperatures in spring [51]. Such a shift towards the beginning of the year is especially observed for RCP8.5 for the far future scenarios and needs to be compensated by higher developmental rates during later phenological growth stages in order to reach maturity [7]. The current study indicates a significant impact of global change on WOSR production in Luxembourg. On average, a shift towards an earlier onset of approximately 7 days for the two future periods in comparison to the reference timespan was detected. This shift in phenology is in line with results from the literature. In an earlier study, Junk et al. [20] have shown that the onset of the growth stage of stem elongation of WOSR occurs between 3.0 and 3.3 days earlier per decade under future climate conditions.

Twenty-three different cultivars of WOSR (8 open-pollinating and 15 hybrid cultivars) were grown on the different test sites including the individual rate of development and temperature sensitivity. The identification of WOSR varieties with a phenological development later in the season might play an important role in agriculture in order to reduce the

effect of low temperatures or late frost events [7]. More data would be necessary for the selection of suitable varieties for adaptive management strategies.

Due to climate change the use of tailored decision support tools for precision agriculture is becoming of even more importance. Increased future variability of meteorological parameters will result in higher uncertainties for yield and biomass production as well as economic income for farmers [52]. WOSR is an important element in crop rotations, which are highly affecting the amount of insect pests as well as the outbreak of plant diseases. Nevertheless, with the high requirements of WOSR towards fertilizers and pesticides, ecological intensification is only possible via smart solutions like decision support tools for appropriate timing of agricultural management steps. Therefore, we proposed such an approach for predicting important growth stages of WOSR, enabling the farmer a better timing for chemical pest control. Our model approach was able to predict the beginning of inflorescence emergence, flowering and end of flowering with low uncertainties comparable to other studies from the literature. Further work is required to cover the whole model chain from the phenological development of WOSR until real yield forecasts under future climate conditions. Additionally, previous studies have indicated that calibration of WOSR phenology from one location/country might be used for more global applications [53].

5. Conclusions

In conclusion, our study presents a comprehensive set of statistical models tailored for predicting specific phenological stages of WOSR cultivation in Luxembourg. Leveraging extensive field observations and corresponding meteorological data, our models accurately forecasted inflorescence emergence, initial flowering, and cessation of flowering, highlighting the pivotal role of accumulated heat units and identifying an optimal temperature range crucial for phenological development. Our findings contribute to a better understanding of WOSR growth dynamics under current and future climate conditions. Evaluation via the PMP5.5 modeling platforms showcased promising results, with our model outperforming comparable studies and exhibiting particular performance in predicting critical growth stages relevant to pest control.

However, challenges persist, notably in predicting late-stage phenological events influenced by leaf senescence. These challenges underscore the necessity for cultivar selection strategies attuned to temperature sensitivities and the adoption of tailored decision support tools to mitigate associated risks.

In the face of escalating climate variability, precision agriculture emerges as a cornerstone for sustainable WOSR cultivation, offering avenues for ecological intensification while optimizing resource allocation. Our study advocates for the proactive integration of predictive modeling into adaptive management frameworks, empowering stakeholders to navigate evolving climatic conditions and safeguard the resilience of WOSR production systems in Luxembourg and beyond.

Author Contributions: Conceptualization, J.J. and M.E.; methodology, A.T. and M.E.J.; validation, J.J.; formal analysis, A.T. and M.E.; writing—original draft preparation, J.J.; writing—review and editing, A.T. and M.E.; funding acquisition, J.J. All authors have read and agreed to the published version of the manuscript.

Funding: Parts of the research was funded by the Ministry of the Environment, Climate and Biodiversity (MECB) of Luxembourg, in the framework of the CHAPEL project (<https://www.list.lu/en/environment/project/chapel/>, accessed on 15 May 2024) as well by the by the Ministry of Agriculture, Food and Viticulture in the framework of the SENTINELLE project.

Institutional Review Board Statement: Not applicable.

Data Availability Statement: The observation meteorological data from the ASTA station can be downloaded from <https://www.agrimeteo.lu/> (accessed on 15 May 2024). The field observations of the individual BBCH stages are available on request from the corresponding authors. The CORDEX regional climate model data are available from the Copernicus Climate Data Store, <https://doi-org.proxy.bnl.lu/10.24381/cds.bc91edc3> (accessed on 15 May 2024).

Conflicts of Interest: The authors declare no conflicts of interest. The funders had no role in the design of the study; in the collection, analyses, or interpretation of data; in the writing of the manuscript; or in the decision to publish the result.

Appendix A

XML file of the PMP5.5 model configuration for the BBCH stage 51.

Appendix B

XML file of the PMP5.5 model configuration for the BBCH stage 60.

Appendix C

XML file of the PMP5.5 model configuration for the BBCH stage 69.

References

- European Commission, DG Agriculture and Rural Development. *EU agricultural Outlook for Markets, Income and Environment, 2021–2031*; European Commission, DG Agriculture and Rural Development: Brussels, Belgium, 2021; p. 83.
- Junk, J.; Ulber, B.; Vidal, S.; Eickermann, M. Assessing climate change impacts on the rape stem weevil, *Ceutorhynchus napi* Gyll., based on bias- and non-bias-corrected regional climate change projections. *Int. J. Biometeorol.* **2015**, *59*, 1597–1605. [[CrossRef](#)] [[PubMed](#)]
- Böttcher, U.; Rampin, E.; Hartmann, K.; Zanetti, F.; Flenet, F.; Morison, M.; Kage, H. A phenological model of winter oilseed rape according to the BBCH scale. *Crop Pasture Sci.* **2016**, *67*, 345–358. [[CrossRef](#)]
- Hegewald, H.; Koblenz, B.; Wensch-Dorendorf, M.; Christen, O. Yield, yield formation, and blackleg disease of oilseed rape cultivated in high-intensity crop rotations. *Arch. Agron. Soil Sci.* **2017**, *63*, 1785–1799. [[CrossRef](#)]
- Hegewald, H.; Wensch-Dorendorf, M.; Sieling, K.; Christen, O. Impacts of break crops and crop rotations on oilseed rape productivity: A review. *Eur. J. Agron.* **2018**, *101*, 63–77. [[CrossRef](#)]
- Williams, I.H. *Biocontrol-Based Integrated Management of Oilseed Rape Pests*; Springer: Dordrecht, The Netherlands, 2010.
- Pullens, J.W.M.; Sharif, B.; Trnka, M.; Balek, J.; Semenov, M.A.; Olesen, J.E. Risk factors for European winter oilseed rape production under climate change. *Agric. For. Meteorol.* **2019**, *272–273*, 30–39. [[CrossRef](#)]
- Drebenstedt, I.; Schmid, I.; Poll, C.; Marhan, S.; Kahle, R.; Kandeler, E.; Högy, P. Effects of soil warming and altered precipitation patterns on photosynthesis, biomass production and yield of barley. *J. Appl. Bot. Food Qual.* **2020**, *93*, 44–53. [[CrossRef](#)]
- Junk, J.; Jonas, M.; Eickermann, M. Assessing meteorological key factors influencing crop invasion by pollen beetle (*Meligethes aeneus* F.)—past observations and future perspectives. *Meteorol. Z.* **2015**, *25*, 357–364. [[CrossRef](#)]
- IPCC. *Climate Change 2007: The Physical Science Basis: Contribution of Working Group I to the Fourth Assessment Report of the Intergovernmental Panel on Climate Change*; Cambridge University Press: Cambridge, UK, 2007.
- Olesen, J.E.; Trnka, M.; Kersebaum, K.C.; Skjelvåg, A.O.; Seguin, B.; Peltonen-Sainio, P.; Rossi, F.; Kozyra, J.; Micale, F. Impacts and adaptation of European crop production systems to climate change. *Eur. J. Agron.* **2011**, *34*, 96–112. [[CrossRef](#)]
- Marini, L.; St-Martin, A.; Vico, G.; Baldoni, G.; Berti, A.; Blecharczyk, A.; Malecka-Jankowiak, I.; Morari, F.; Sawinska, Z.; Bommarco, R. Crop rotations sustain cereal yields under a changing climate. *Environ. Res. Lett.* **2020**, *15*, 124011. [[CrossRef](#)]
- Borges, C.E.; Von Dos Santos Veloso, R.; da Conceicao, C.A.; Mendes, D.S.; Ramirez-Cabral, N.Y.; Shabani, F.; Shafapourtehrany, M.; Nery, M.C.; da Silva, R.S. Forecasting *Brassica napus* production under climate change with a mechanistic species distribution model. *Sci. Rep.* **2023**, *13*, 12656. [[CrossRef](#)]
- Junk, J.; Sulis, M.; Trebs, I.; Torres-Matallana, J.A. Evaluating the Present and Future Heat Stress Conditions in the Grand Duchy of Luxembourg. *Atmosphere* **2024**, *15*, 112. [[CrossRef](#)]
- Junk, J.; Goergen, K.; Krein, A. Future Heat Waves in Different European Capitals Based on Climate Change Indicators. *Int. J. Environ. Res. Public Health* **2019**, *19*, 3959. [[CrossRef](#)] [[PubMed](#)]
- Eickermann, M.; Junk, J.; Rapisarda, C. Climate Change and Insects. *Insects* **2023**, *14*, 678. [[CrossRef](#)] [[PubMed](#)]
- Santos, J.A.; Fraga, H.; Malheiro, A.C.; Moutinho-Pereira, J.; Dinis, L.-T.; Correia, C.; Moriondo, M.; Leolini, L.; Dibari, C.; Costafreda-Aumedes, S.; et al. A Review of the Potential Climate Change Impacts and Adaptation Options for European Viticulture. *Appl. Sci.* **2020**, *10*, 3092. [[CrossRef](#)]
- Goergen, K.; Beersma, J.; Hoffmann, L.; Junk, J. ENSEMBLES-based assessment of regional climate effects in Luxembourg and their impact on vegetation. *Clim. Chang.* **2013**, *119*, 761–773. [[CrossRef](#)]
- Habekotté, B. Evaluation of seed yield determining factors of winter oilseed rape (*Brassica napus* L.) by means of crop growth modelling. *Field Crops Res.* **1997**, *54*, 137–151. [[CrossRef](#)]
- Junk, J.; Eickermann, M.; Görgen, K.; Beyer, M.; Hoffmann, L. Ensemble-based analysis of regional climate change effects on the cabbage stem weevil (*Ceutorhynchus pallidactylus* (Mrsh.)) in winter oilseed rape (*Brassica napus* L.). *J. Agric. Sci.* **2012**, *150*, 191–202. [[CrossRef](#)]
- Cuccia, C.; Bois, B.; Richard, Y.; Parker, A.K.; Garcia De Cortazar-Ataauri, I.; Van Leewen, C.; Castel, T. Phenological model performance to warmer conditions: Application to Pinot Noir in Burgundy. *J. Int. Sci. Vigne Vin* **2014**, *48*, 169–178.

22. García de Cortázar-Atauri, I.; Brisson, N.; Gaudillere, J.P. Performance of several models for predicting budburst date of grapevine (*Vitis vinifera* L.). *Int. J. Biometeorol.* **2009**, *53*, 317–326. [[CrossRef](#)]
23. Duchêne, E.; Huard, F.; Dumas, V.; Schneider, C.; Merdinoglu, D. The challenge of adapting grapevine varieties to climate change. *Clim. Res.* **2010**, *41*, 193–204. [[CrossRef](#)]
24. Leolini, L.; Costafreda-Aumedes, S.; Santos, J.A.; Menz, C.; Fraga, H.; Molitor, D.; Merante, P.; Junk, J.; Kartschall, T.; Destrac-Irvine, A.; et al. Phenological Model Intercomparison for Estimating Grapevine Budbreak Date (*Vitis vinifera* L.) in Europe. *Appl. Sci.* **2020**, *10*, 3800. [[CrossRef](#)]
25. Chuine, I.; de Cortazar-Atauri, I.G.; Kramer, K.; Hänninen, H. Plant Development Models. In *Phenology: An Integrative Environmental Science*; Schwartz, M.D., Ed.; Springer: Dordrecht, The Netherlands, 2013; pp. 275–293.
26. Alford, D.V.; Nilsson, C.; Ulber, B. Insect pests of oilseed rape crops. In *Biocontrol of Oilseed Rape Pests*; Alford, D.V., Ed.; Blackwell Science: Oxford, UK, 2003; pp. 9–41.
27. Nilsson, C. Yield losses in summer rape caused by pollen beetles (*Meligethes* spp.). *Swed. J. Agric. Res.* **1987**, *17*, 105–111.
28. Eickermann, M.; Delfosse, P.; Hoffmann, L.; Beyer, M. A note on the insecticide sensitivity status of *Meligethes* species (Coleoptera: Nitidulidae) in Luxembourg. *J. Plant Dis. Prot.* **2011**, *118*, 134–140. [[CrossRef](#)]
29. Nedić, N.; Mačukanović-Jocić, M.; Rančić, D.; Rørslett, B.; Šošarić, I.; Stevanović, Z.D.; Mladenović, M. Melliferous potential of *Brassica napus* L. subsp. *napus* (Cruciferae). *Arthropod-Plant Interact.* **2013**, *7*, 323–333. [[CrossRef](#)]
30. Brandt, A.; Gorenflo, A.; Siede, R.; Meixner, M.; Büchler, R. The neonicotinoids thiacloprid, imidacloprid, and clothianidin affect the immunocompetence of honey bees (*Apis mellifera* L.). *J. Insect Physiol.* **2016**, *86*, 40–47. [[CrossRef](#)] [[PubMed](#)]
31. Habekotté, B. A model of the phenological development of winter oilseed rape (*Brassica napus* L.). *Field Crops Res.* **1997**, *54*, 127–136. [[CrossRef](#)]
32. Gabrielle, B.; Denoroy, P.; Gosse, G.; Justes, E.; Andersen, M. A model of leaf area development and senescence for winter oilseed rape. *Field Crops Res.* **1998**, *57*, 209–222. [[CrossRef](#)]
33. Gilardelli, C.; Stella, T.; Frasso, N.; Cappelli, G.; Bregaglio, S.; Chiodini, M.; Scaglia, B.; Confalonieri, R. WOFOST-GTC: A new model for the simulation of winter rapeseed production and oil quality. *Field Crops Res.* **2016**, *197*, 125–132. [[CrossRef](#)]
34. Meier, U. *Growth Stages of Mono- and Dicotyledonous Plants—BBCH Monograph*; Julius Kühn-Institut (JKI): Quedlinburg, Germany, 2018.
35. Lancashire, P.D.; Bleiholder, H.; Boom, T.v.d.; Langelüddeke, P.; Stauss, R.; Weber, E.; Witzemberger, A. A uniform decimal code for growth stages of crops and weeds. *Ann. Appl. Biol.* **1991**, *119*, 561–601. [[CrossRef](#)]
36. Hempel, S.; Frieler, K.; Warszawski, L.; Schewe, J.; Piontek, F. A trend-preserving bias correction—the ISI-MIP approach. *Earth Syst. Dyn.* **2013**, *4*, 219–236. [[CrossRef](#)]
37. Cannon, A.J. Multivariate quantile mapping bias correction: An N-dimensional probability density function transform for climate model simulations of multiple variables. *Clim. Dyn.* **2017**, *50*, 31–49. [[CrossRef](#)]
38. Core-Team, R. *R: A Language and Environment for Statistical Computing*; R Foundation for Statistical Computing: Vienna, Austria, 2023.
39. Gudmundsson, L.; Bremnes, J.B.; Haugen, J.E.; Engen-Skaugen, T. Technical Note: Downscaling RCM precipitation to the station scale using statistical transformations—a comparison of methods. *Hydrol. Earth Syst. Sci.* **2012**, *16*, 3383–3390. [[CrossRef](#)]
40. Metropolis, N.; Rosenbluth, A.W.; Rosenbluth, M.N.; Teller, A.H.; Teller, E. Equation of state calculations by fast computing machines. *J. Chem. Phys.* **1953**, *21*, 1087–1092. [[CrossRef](#)]
41. Hänninen, H. Modeling Dormancy Release in Trees from Cool and Temperate Regions. In *Process Modeling of Forest Growth Responses to Environmental Stress*; Dixon, R.K., Meldahl, R.S., Ruark, G.A., Warren, W.G., Eds.; Timber Press, Inc.: Portland, Oregon, 1990; pp. 159–165.
42. Richardson, E.A. A model for estimating the completion of rest for Redheaven and Elberta peach trees. *Hortic. Sci.* **1974**, *9*, 311–312.
43. Chuine, I.; Beaubien, E.G. Phenology is a major determinant of tree species range. *Ecol. Lett.* **2001**, *4*, 500–510. [[CrossRef](#)]
44. Wong, T.-T. Performance evaluation of classification algorithms by k-fold and leave-one-out cross validation. *Pattern Recognit.* **2015**, *48*, 2839–2846. [[CrossRef](#)]
45. Marshall, B.; Squire, G.R. Non-linearity in rate-temperature relations of germination in oilseed rape. *J. Exp. Bot.* **1996**, *47*, 1369–1375. [[CrossRef](#)]
46. Farré, I.; Robertson, M.; Asseng, S. Reliability of canola production in different rainfall zones of Western Australia. *Aust. J. Agric. Res.* **2007**, *58*, 326–334. [[CrossRef](#)]
47. Müller, J.; Diepenbrock, W. Measurement and modelling of gas exchange of leaves and pods of oilseed rape. *Agric. For. Meteorol.* **2006**, *139*, 307–322. [[CrossRef](#)]
48. Morrison, M.J.; Stewart, D.W.; McVetty, P.B.E. Maximum area, expansion rate and duration of summer rape leaves. *Can. J. Plant Sci.* **1991**, *72*, 117–126. [[CrossRef](#)]
49. Bennett, E.J.; Roberts, J.A.; Wagstaff, C. The role of the pod in seed development: Strategies for manipulating yield. *New Phytol.* **2011**, *190*, 838–853. [[CrossRef](#)] [[PubMed](#)]
50. Bamminger, C.; Poll, C.; Sixt, C.; Högy, P.; Wüst, D.; Kandeler, E.; Marhan, S. Short-term response of soil microorganisms to biochar addition in a temperate agroecosystem under soil warming. *Agric. Ecosyst. Environ.* **2016**, *233*, 308–317. [[CrossRef](#)]

51. Rapacz, M.; Markowski, A. Winter Hardiness, Frost Resistance and Vernalization Requirement of European Winter Oilseed Rape (*Brassica napus* var. *oleifera*) Cultivars within the Last 20 Years. *J. Agron. Crop Sci.* **1999**, *183*, 243–253. [[CrossRef](#)]
52. El Jarroudi, M.; Kouadio, L.; Bock, C.; El Jarroudi, M.; Junk, J.; Pasquali, M.; Maraite, H.; Delfosse, P. A threshold-based weather model for predicting stripe rust infection in winter wheat. *Plant Dis.* **2017**, *101*, 693–703. [[CrossRef](#)]
53. Wang, E.; Engel, T. Simulation of phenological development of wheat crops. *Agric. Syst.* **1998**, *58*, 1–24. [[CrossRef](#)]

Disclaimer/Publisher’s Note: The statements, opinions and data contained in all publications are solely those of the individual author(s) and contributor(s) and not of MDPI and/or the editor(s). MDPI and/or the editor(s) disclaim responsibility for any injury to people or property resulting from any ideas, methods, instructions or products referred to in the content.